NOTES AND CORRESPONDENCE

The Motion of a Turbulent Thermal in the Presence of Background Rotation

BARBARA ANNE AYOTTE AND HARINDRA J. S. FERNANDO

Environmental Fluid Dynamics Program, Department of Mechanical and Aerospace Engineering, Arizona State University, Tempe, Arizona

15 March 1993 and 11 October 1993

Thermals are buoyant fluid parcels instantly released from a source. Since the pioneering work of Scorer (1957), the flow field associated with thermals has been subjected to detailed theoretical, numerical, and experimental investigations; some recent references are Telford (1988), Lundgren et al. (1992), and Johari (1992), respectively. In an atmospheric context, thermals are of importance in studies related to such phenomena as the formation and growth of cumulus clouds and the generation of wind shear by the impact on the ground of descending cold air masses from thunderstorm outflows. Although a considerable amount of work has been reported on the motion of thermals in neutral and stratified environments, to our knowledge, the only published laboratory study on the influence of background rotation (e.g., earth's Coriolis forces or presence of a parent cyclone) on their motion is by Wilkins et al. (1969). In this study, however, the buoyant fluid mass was injected as a turbulent puff; hence, its behavior is expected to be different from a simple thermal. In addition, the effects of rotation on the growth of turbulent length scales were not considered. On the other hand, the general aspects related to the influence of rotation on axisymmetric jets and plumes have been discussed previously (e.g., Turner and Lilly 1963; Niino 1980). Here we report the results of a laboratory study and relevant scaling analysis on the influence of background rotation on the motion of a thermal, for the case where the direction of the thermal motion and the rotational vector are in the same direction.

Corresponding author address: Prof. Harindra J. Fernando, Dept. of Mechanical and Aerospace Engineering, Arizona State University, Tempe, AZ 85287-6106.

The experiments were conducted in a tank of dimensions 60 × 60 × 60 (cm) mounted on a rotating table (Fig. 1). The tank was filled with freshwater to a depth of 50 cm, and the thermal-producing mechanism was placed at the center just below the water surface. A thermal was produced by momentarily releasing a fixed mass of dense salty water of density ρ_T from a flat-bottomed funnel. This fluid was colored with fluorescein dye to facilitate flow visualization and the flow field was illuminated by an arc lamp from the side against a black backdrop. The motion of the thermal was monitored by using video and still cameras. The background fluid was homogeneous (density ρ_0), so that the initial total buoyancy of the fluid can be calculated as $q_T = V_0(\rho_T - \rho_0)g/\rho_0$, where g is the gravitational acceleration and V_0 is the initial volume of the thermal. Several initial volumes $V_0 = 5-15$ cm^3 were used with densities in the range 1.005–1.05 g cm^{-3}. It is possible to show that the Reynolds number Re of the thermal, based on the descent velocity of the cap V_d and the visual diameter of the thermal d, Re $= V_d d/\nu$, where ν is the kinematic viscosity, is Re $\approx 1.5\ q_T^{1/2}/\nu$ (Scorer 1957; Johari 1992). Accordingly, the characteristic Reynolds number for the present experiments is in the order of 2500, which is the same as that of Scorer's (1957) experiments. The Re values used were sufficient to ensure that the thermals are turbulent.

Initially the tank was filled with homogeneous water and then was spun up to the desired speed. The background rate of rotation Ω was varied in the range $0.3 < \Omega < 0.7$ rad s^{-1}. After rotating for about 1 1/2 hours, the thermal was discharged. The descending, illuminated, thermal was videotaped and was later analyzed frame by frame to measure its growth characteristics: that is, the distance traveled by the bottom of the plume cap from the point of release and the maximum width

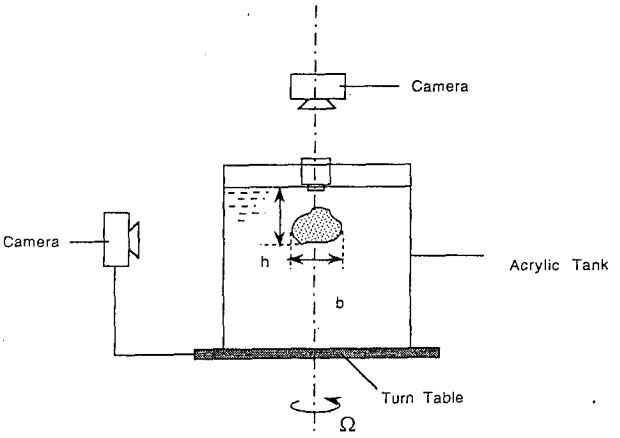

FIG. 1. A schematic of the experimental apparatus.

in the lateral direction (i.e., perpendicular to the axis of rotation). These were read directly from a video screen, and the size of the thermal was obtained using a scale attached to the tank. The boundaries of the thermal were very sharp, and obtaining data by this method is expected to be reasonably accurate; this was ensured by image processing some video frames to calculate the width of the thermal and comparing the results with those obtained by visual means.

During descent the thermal was initially found to accelerate for a short distance (4–6 cm), and then, upon quickly achieving a maximum speed, decelerate continuously. Previous (self-similarity) arguments and laboratory experiments (Scorer 1957; Sanchez et al. 1989) suggest that, in the absence of background rotation, the visual vertical distance traveled by the thermal cap h and its lateral maximum width b, should satisfy at any time t during the decelerating phase,

$$h = c_1 q_T^{1/4} t^{1/2}, \tag{1}$$

$$b = c_2 h, \tag{2}$$

where c_1, c_2 are constants. The present experiments show that (1) and (2) are also followed approximately with $c_1 \approx 1.8$ and $c_2 \approx 0.33$ in the initial phase of descent. However, after some time, the lateral growth of the thermal stops, indicating the onset of rotational effects. Figure 2 shows a series of photographs that depict the initial growth of the thermal, which is followed by a period of descent with no lateral growth.

Figures 3 and 4 show normalized plots of b and h versus t. Note the initial increase of b and the inhibition of growth after some time; interestingly enough, the vertical propagation of the thermal continued but at a slightly reduced speed. Since the thermal attains its maximum horizontal size gradually, it is difficult to estimate the exact time t_c at which the rotation becomes important. Estimates of t_c were made by determining the intersection point of the best-fit straight line with a unit slope to log$b$ versus $\log(t^{1/2})$ data, for $0.5 < \Omega t < 1$, and b = const line, for $\Omega t > 2$; see Fig. 3. The data of 12 different runs revealed that $\Omega t_c \approx 1.62 \pm 0.2$ (SD), where SD represents the standard deviation.

It is possible to argue that the inhibition of the horizontal growth of the thermal occurs when the turbulence within the patch is arrested by the rotational (Coriolis) effects, which exert a restraining force on the turbulent fluid motion inside the thermals; this force acts perpendicular to the axis of rotation. If the characteristic rms velocity and integral lengthscale of turbulence within the thermal can be written as u and l, respectively, then an expression can be obtained for the vertical distance traveled h_c and the corresponding width b_c of the thermal whence the rotational influence becomes important. The basis of this expression is that the inertial forces of the energy-containing turbulent eddies ($\sim u^2/l$) come to a balance with the Coriolis forces ($\sim 2\Omega u$) (e.g., Fernando et al. 1991). If it is assumed that the thermal motion in the absence of rotation is determined by the sole parameter q_T (cf. Turner 1979), then it is possible to argue that $u = u(q_T, t) = u(q_T, h) \sim (q_T/h^2)^{1/2}$ and $l \sim h \sim b$. Thus, the width b_c of the thermal at the onset of rotational effects can be written as

$$b_c = c_3 (q_T/\Omega^2)^{1/4}, \tag{3}$$

where c_3 is a constant. Figure 5 shows a plot of b_c versus $(q_T/\Omega^2)^{1/4}$; good agreement can be seen between the prediction and the results. A best-fit line to the graph indicates a slope of 0.96, and the forced-fit line with unit slope indicates $c_3 \approx 0.9$. Since the thermal satisfies (2) before the onset of rotational effects, it is expected that

$$h_c = c_4 (q_T/\Omega^2)^{1/4}, \tag{4}$$

where c_4 is a constant. Figure 6 shows the distance traveled by the thermal h_c at the onset of rotational effects. The data showed an increasing trend with $(q_T/\Omega^2)^{1/4}$, but the slope of the best-fit line is somewhat less than unity (i.e., 0.8); a forced-fit line with unit slope showed $c_4 \approx 2.3$.

FIG. 2. Photographs depicting the evolution of thermals in the presence of background rotation; the nondimensional times (Ωt) at which the photographs were taken are also shown.

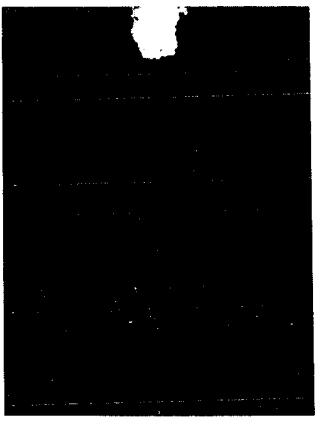

$\Omega t = 0.09$

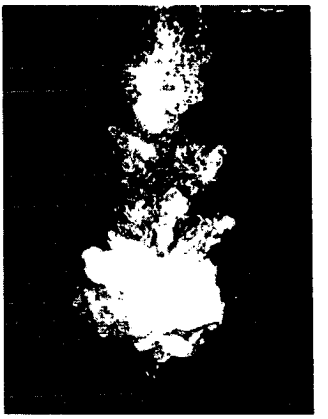

$\Omega t = 1.41$

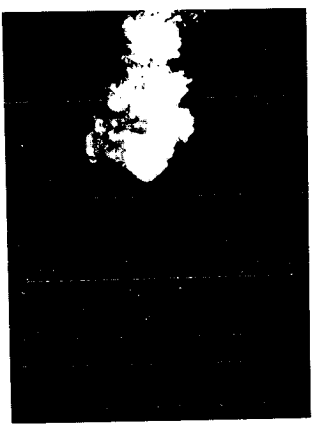

$\Omega t = 0.52$

$\Omega t = 2.08$

$\Omega t = 1.04$

$\Omega t = 16.6$

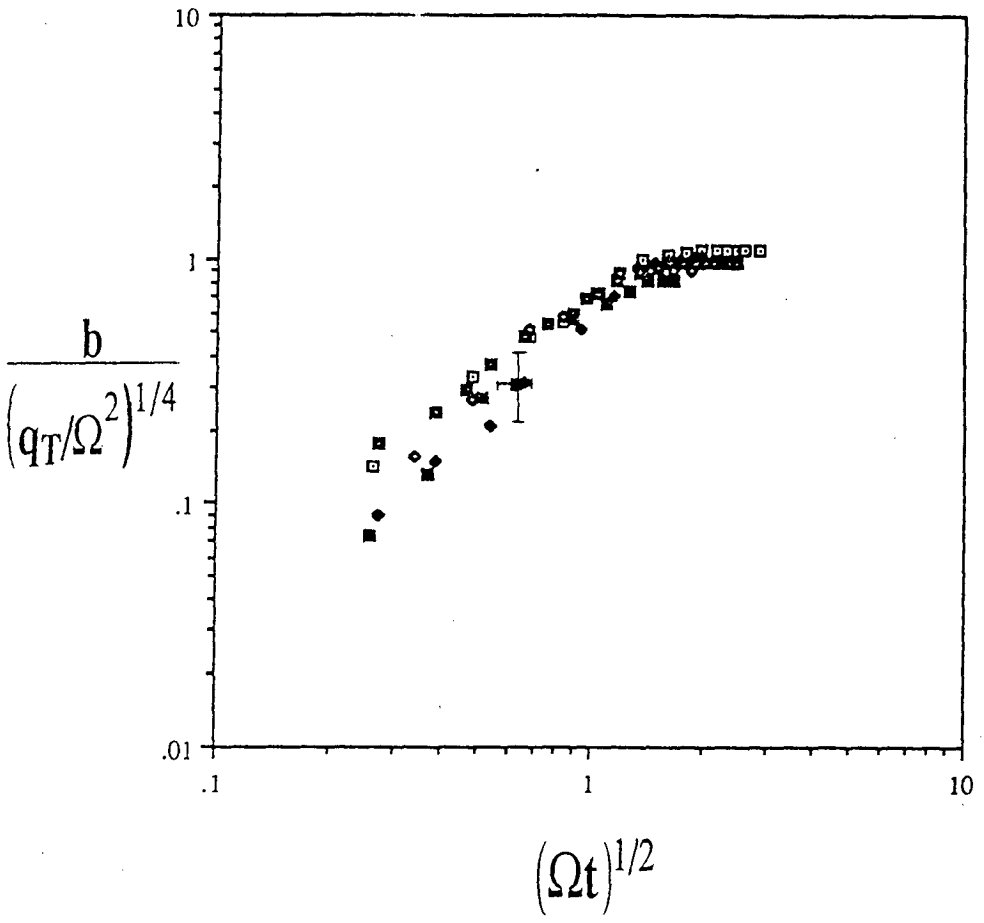

FIG. 3. A plot of the dimensionless width of the thermal versus dimensionless time. Open square with dot: $V_0 = 5$ cm^3, $\Omega = 0.7$ rad s^{-1}, $\Delta b = 58.9$ cm s^{-2}; solid diamond: $V_0 = 10$ cm^3, $\Omega = 0.44$ rad s^{-1}, $\Delta b = 58.9$ cm s^{-2}; open square: $V_0 = 5$ cm^3; $\Omega = 0.44$ rad s^{-1}, $\Delta b = 58.9$ cm s^{-2}; open diamond: $V_0 = 10$ cm^3; $\Omega = 0.7$ rad s^{-1}, $\Delta b = 9.8$ cm s^{-2}; solid square: $V_0 = 15$ cm^3; $\Omega = 0.4$ rad s^{-1}, $\Delta b = 78.5$ cm s^{-2}.

If the descent of the thermal follows (1) and (2), with $c_3 \approx 0.9$ and $c_2 \approx 0.33$, in the proximity of the onset of rotational effects, then $c_4 = c_3/c_2 \approx 2.7$, which is somewhat higher than that obtained by direct measurements; the gradual reduction of the speed of descent of the thermal near t_c explains this discrepancy. Beyond t_c, the growth in the radial direction is inhibited by the background rotation, but its effect on the rate of descent appears to be small.

It is instructive to apply the above results to investigate the possibility of atmospheric thermals becoming affected by the earth's Coriolis forces. It should be cautioned that atmospheric thermals are subjected to a number of effects such as condensation of water vapor within the thermal (which produce additional buoyancy forces), and the presence of cross flow and background turbulence. The thermal "release" mechanism in the atmosphere is also unknown. In addition, at low and midlatitudes the tangential component to the earth of the earth's rotational vector is important, and the growth of the thermal in the vertical as well as horizontal directions can be affected by the Coriolis forces. If this tangential component is not significant and the condensation and ambient forcing are negligible, it is possible to evaluate the typical height a thermal would rise in the atmosphere before the earth's Coriolis forces become important; using the estimated values of buoyancy $(\rho_T - \rho_0)/\rho_0 \sim (1/500)$ and volume (radius ~ 150 m) of atmospheric thermals (Scorer 1957; Woodward 1959) and the typical values of $q_T \approx 2.8 \times 10^5$ m^{4}s^{-2} and $\Omega \approx 7.14 \times 10^{-5}$ rad s^{-1} corresponding to the earth's rate of rotation it is possible to calculate $h_c \approx 2.3(q_T/\Omega^2)^{1/4} \approx 6.25$ km. Thus, only the fluid parcels undergoing atmospheric deep convection

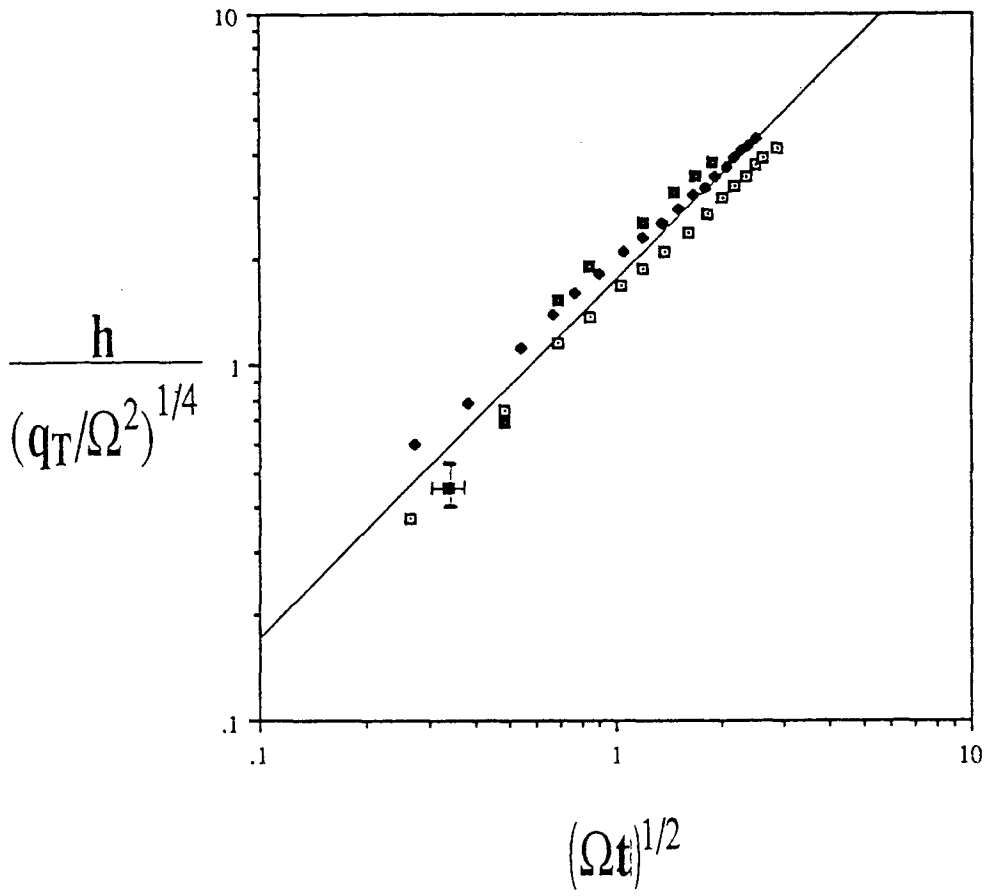

FIG. 4. A plot of the dimensionless distance traveled by the thermal versus dimensionless time. The distance was measured from the location where the thermal was released. Open square with dot: $V_0 = 5$ cm^3, $\Omega = 0.7$ rad s^{-1}, $\Delta b = 58.9$ cm s^{-2}, solid diamond: $V_0 = 5$ cm^3; $\Omega = 0.44$ rad s^{-1}, $\Delta b = 58.9$ cm s^{-2}; open square: $V_0 = 10$ cm^3, $\Omega = 0.7$ rad s^{-1}, $\Delta b = 9.8$ cm s^{-2}

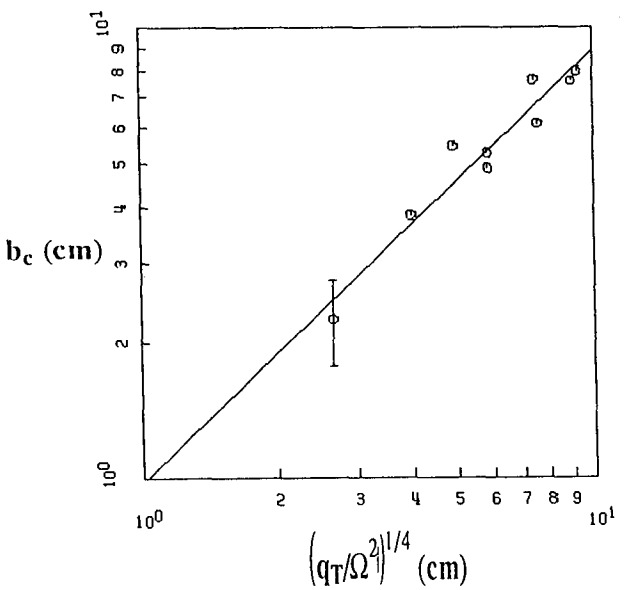

FIG. 5. A plot of the width of the thermal at the onset of the rotational effects b_c versus the length scale $(q_T/\Omega^2)^{1/4}$.

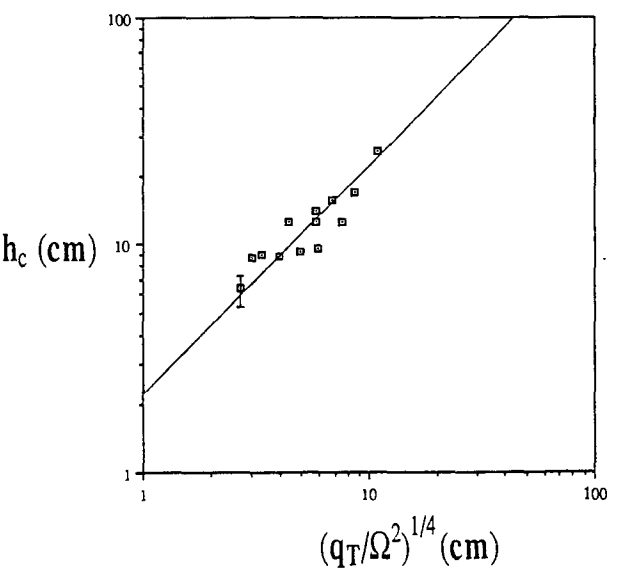

FIG. 6. Same as Fig. 5 but the vertical distance traveled by the thermal h_c is shown.

are expected to be affected by the earth's Coriolis forces. However, if the background rotation is present as a parent cyclone (typical values of Ω for such cases are in the order $10^{-3}\,s^{-1}$), the background rotational effects can come into play at much shorter distances from the release.

Acknowledgments. Stratified and rotating turbulence research at Arizona State University is funded by the Office of Naval Research, the National Science Foundation, and the Environmental Protection Agency. The authors wish to thank Professor D. F. Jankowski for his useful comments and Mr. C. Y. Ching for his technical support, without which this work could not have been completed.

REFERENCES

Fernando, H. J. S., R.-R. Chen, and D. L. Boyer, 1991: Effects of rotation on convective turbulence. *J. Fluid Mech.*, **228,** 513–547.

Johari, H., 1991: Mixing in thermals with and without buoyancy reversal. *J. Atmos. Sci.*, **49,** 1412–1426.

Lundgren, T. S., J. Yao, and N. N. Mansour, 1992: Microburst modelling and scaling. *J. Fluid Mech.*, **239,** 461–488.

Niino, H., 1980: Evolution of a laminar jet in a homogeneous rotating fluid: A linear theory. *J. Meteor. Soc. Japan,* **58,** 33–51.

Sanchez, O., D. J. Raymond, L. Libersky, and A. G. Petschek, 1989: The development of thermal from rest. *J. Atmos. Sci.*, **46,** 2280–2292.

Scorer, R. S., 1957: Experiments on convection of isolated masses of buoyant fluid. *J. Fluid Mech.*, **2,** 583–594.

Telford, J. W., 1988: A theoretical solution to the motion of an atmospheric spherical vortex. *J. Atmos. Sci.*, **45,** 789–802.

Turner, J. S., 1979: *Buoyancy Effects in Fluids.* Cambridge University Press.

——, and D. K. Lilly, 1963: The carbonated tornado vortex. *J. Atmos. Sci.*, **20,** 468–471.

Wilkins, E. M., Y. Sasaki, E. M. Friday, Y. McCarthy, and J. R. McIntyre, 1969: Properties of simulated thermals in a rotating fluid. *J. Geophys. Res.*, **74,** 4472–4486.

Woodward, B., 1959: The motion in and around isolated thermals. *Quart. J. Roy. Meteor. Soc.*, 144–151.